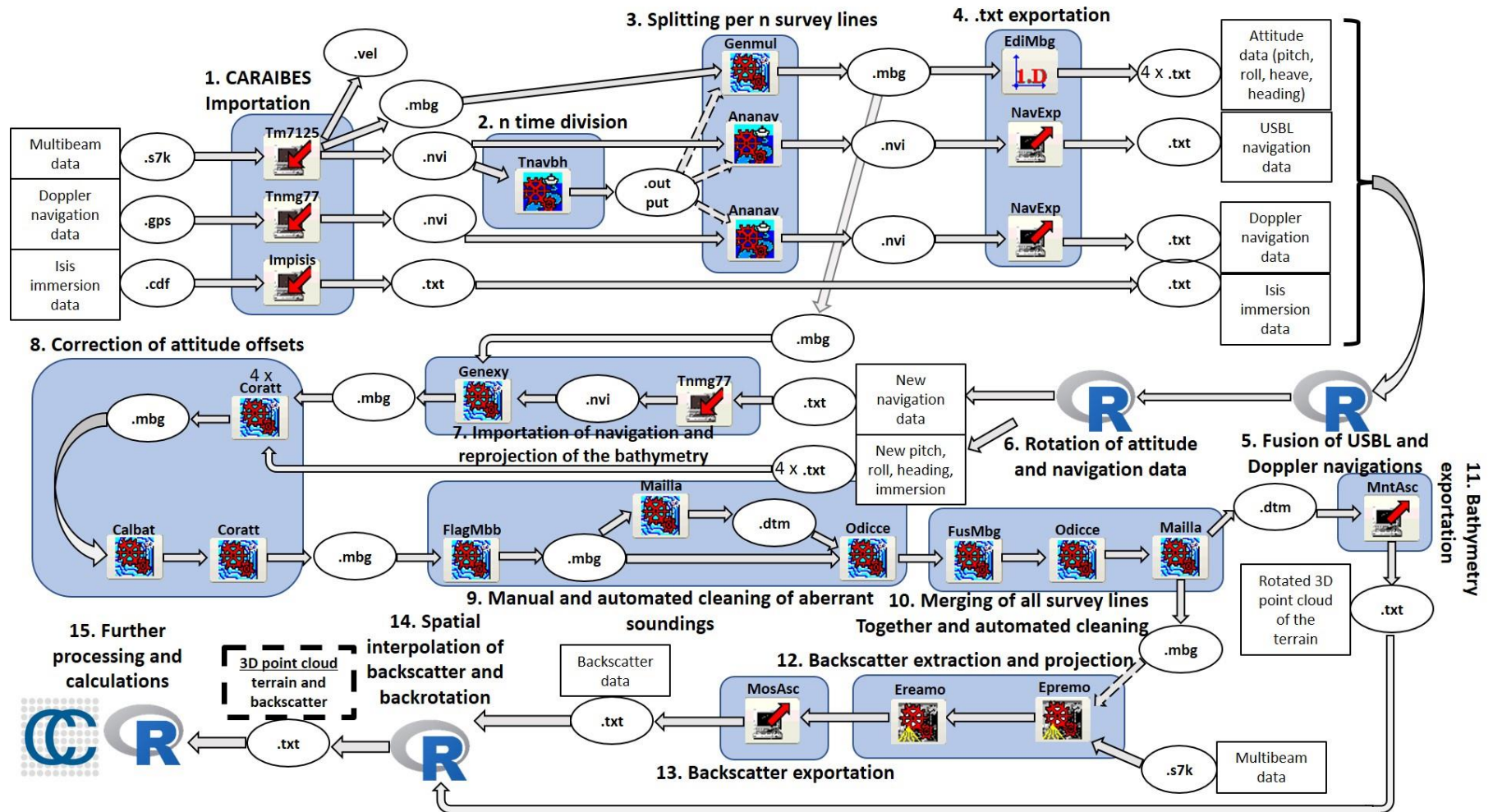


*Supplementary Material*



**Figure S1.** Workflow describing the processing steps achieved in this study to retrieve the terrain and backscatter point cloud of a deep-water vertical wall using a forward-looking multibeam echosounder (MBES; Reson7125) mounted on a ROV and using the software CARAIRES (Ifremer), R (R Core Team,

2013), CloudCompare. Full arrow relays the input/output of a given file from/to a function. Dashed arrow indicates the use of a file as a reference in space or time and needed to perform a function. Light-blue box represents a group of similar processing operations. 1. Importation of sonar and navigation recordings in CARAIBES. 2. Time division based on the time frame of the different survey lines. 3. Splitting of sonar and navigation recordings according to time division files (.output). 4. Navigation exportation in .txt files. 5. Merging of the USBL and Doppler navigations in R. 6. Rotation of attitude parameters and of the corrected navigation data in R to reproject the navigation in a downward-looking configuration. 7. Importation of the rotated navigation and attitude recordings. 8. Correction of attitude parameters offset. 9. Manual and automated cleaning of aberrant soundings (for each survey line separately). 10. Merging of all survey lines together and automated cleaning of aberrant soundings. 11. Bathymetry exportation in point cloud (.txt). 12. Backscatter extraction and projection based on the bathymetry. 13. Exportation of the backscatter (.txt). 14. Spatial interpolation of the backscatter to reposition it onto the bathymetry points, and rotation of the data back to the original coordinate system to create the point cloud. 15. Further derivatives can be calculated in R, CloudCompare and any further analyses can be made.

### Survey line 10

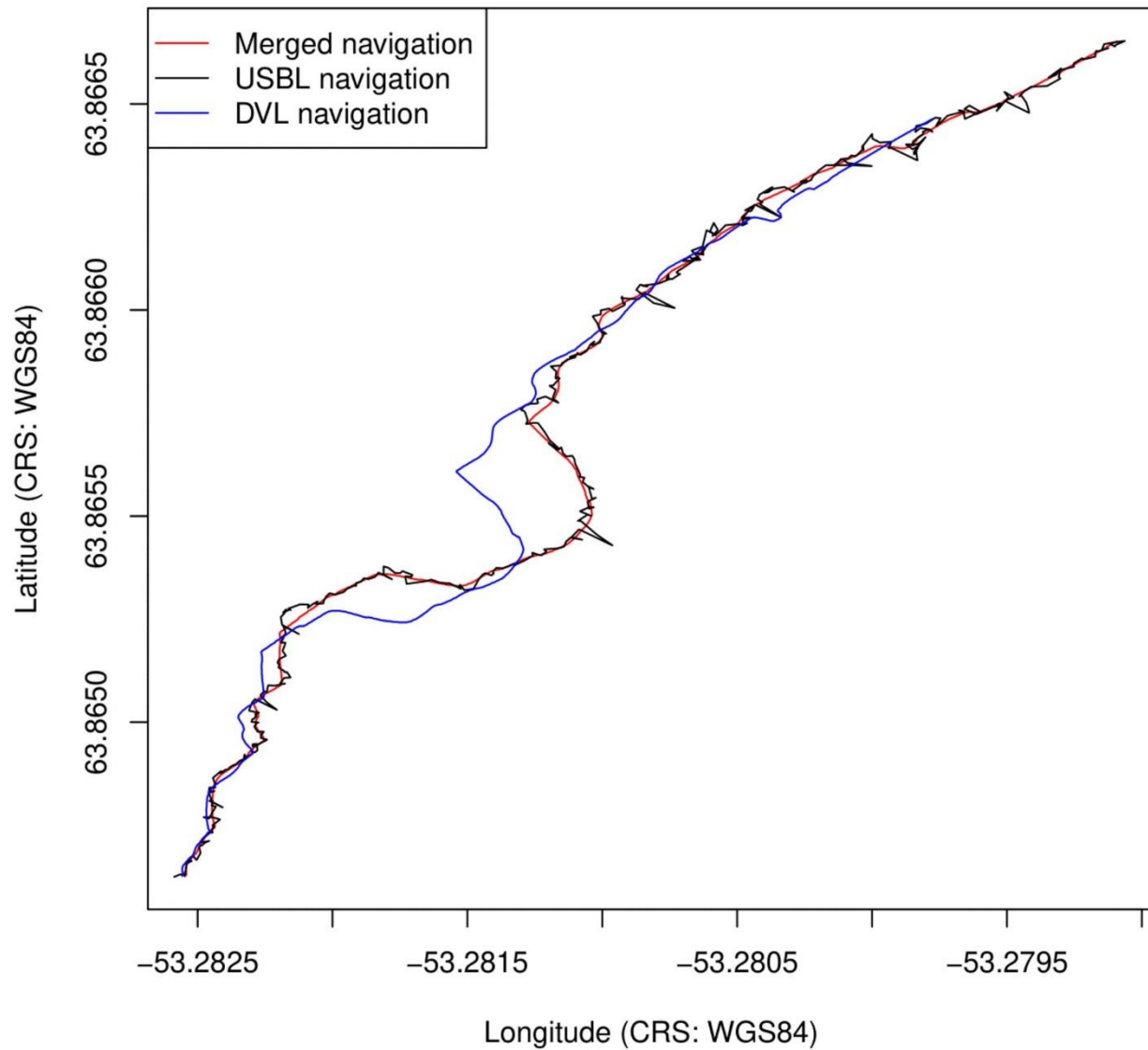


**Figure S2.** Example of the navigation (in red) resulting from the combination of the ‘noisy’ USBL navigation (in black) and the ‘drifting’ DVL navigation (in blue). The merged navigation was computed using a 180-second rolling average of the offset between the USBL and the DVL added to the coordinates of the DVL. This navigation was used to rebuild the terrain of the deep-water cliff using the sonar processing software CARAIBES (Ifremer).

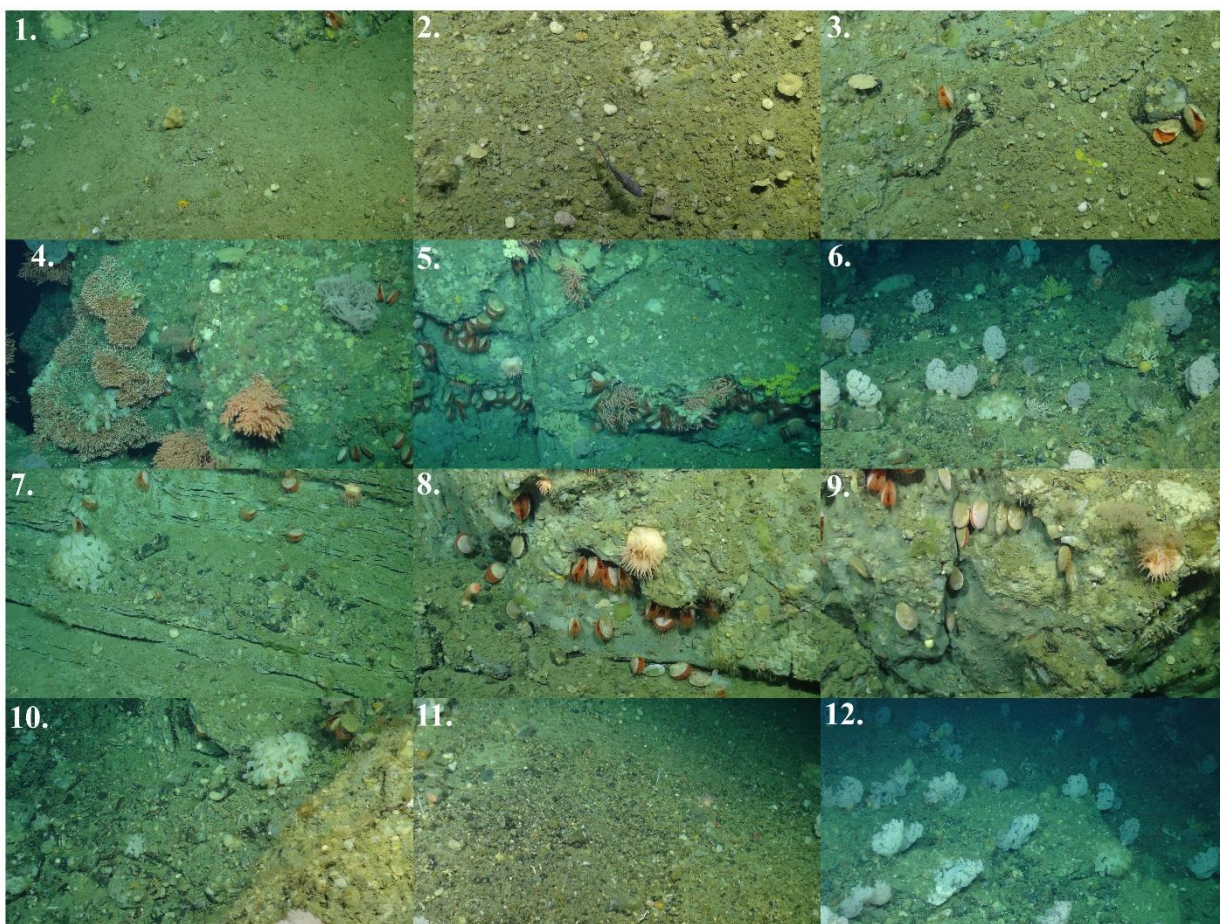
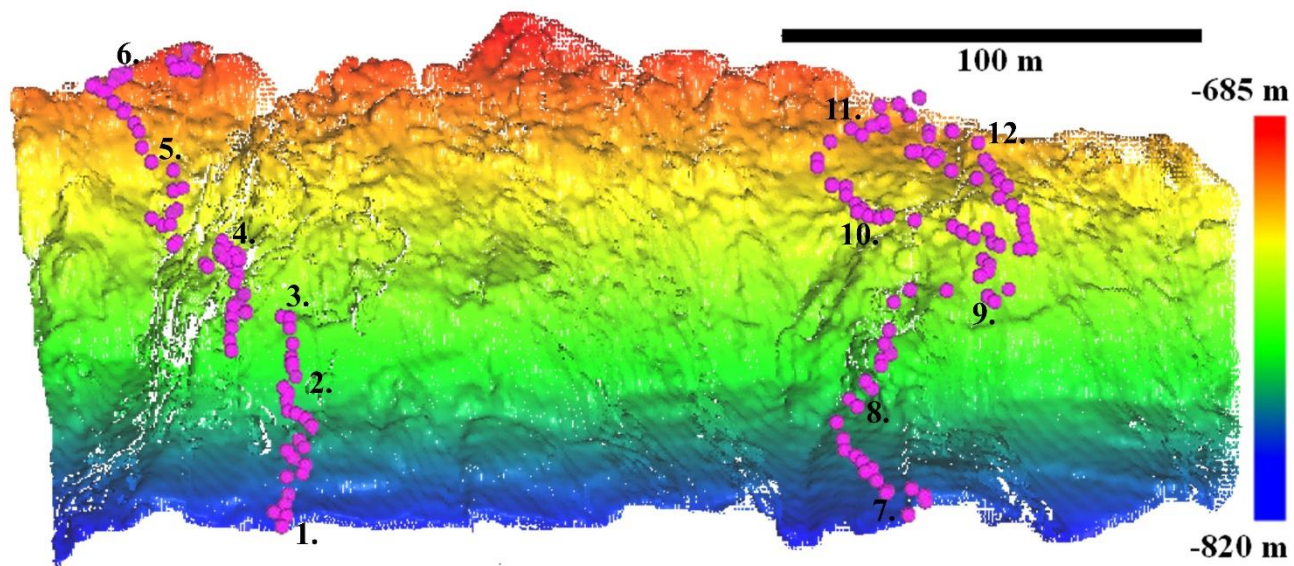


**Figure S3.** High-resolution (0.3 m) terrain point cloud of the underwater wall marking the boundary between a trough and the West Greenland continental shelf ( $63^{\circ}51.9'N$ ,  $53^{\circ}16.9'W$ ). The depth ranges between from -685 m to -820 m and is displayed as a color gradient. The deep-sea cliff terrain was mapped using a forward-

looking MBES mounted onto the ROV Isis (Dive D334) and is displayed as a point cloud using the software CloudCompare. Pink dots locate the position of the ROV when taking seabed groundtruthing pictures (Dive D333) used for the community comparison analysis between abiotic clusters. Numbers position groundtruthing pictures which are displayed below the terrain point cloud. They illustrate different the meter-scale terrain of the underwater wall and coincides with fine-scale features observed in the point cloud. They also host different types of assemblages. 1. Smoother habitat exhibiting some rocks and few sponges spp. 2. Steeper terrain displaying encrusting sponges and a thin layer of sediment. 3. Irregular terrain hosting *Acesta* sp. 4. Rocky outcrops colonized by *Acesta* sp., Hexactinellid and demosponges, *Drifia* sp., *Desmophyllum pertusum*, and *Primnoa resedaeformis*. 5. Irregular terrain supporting increased *Acesta* sp. abundance 6. A shallow mixed coral community dominated by *Drifia* sp. 7. Transition between a smoother (lower image portion) and a steeper hard substrate hosting *Acesta* sp. and Hexactinellid sponges. 8-9. Irregular hard-substrate terrain portions dominated by *Acesta* sp., anemones, and encrusting demosponge. 10. Irregular terrain where rocks and pebbles have accumulated and on which grow Hexactinellid sponges and *Acesta* sp. 11. Smoother terrain covered of pebbles and small *Asbestopluma pennatula*. 12. Flatter terrain supporting a soft coral garden dominated by *Drifia* sp.

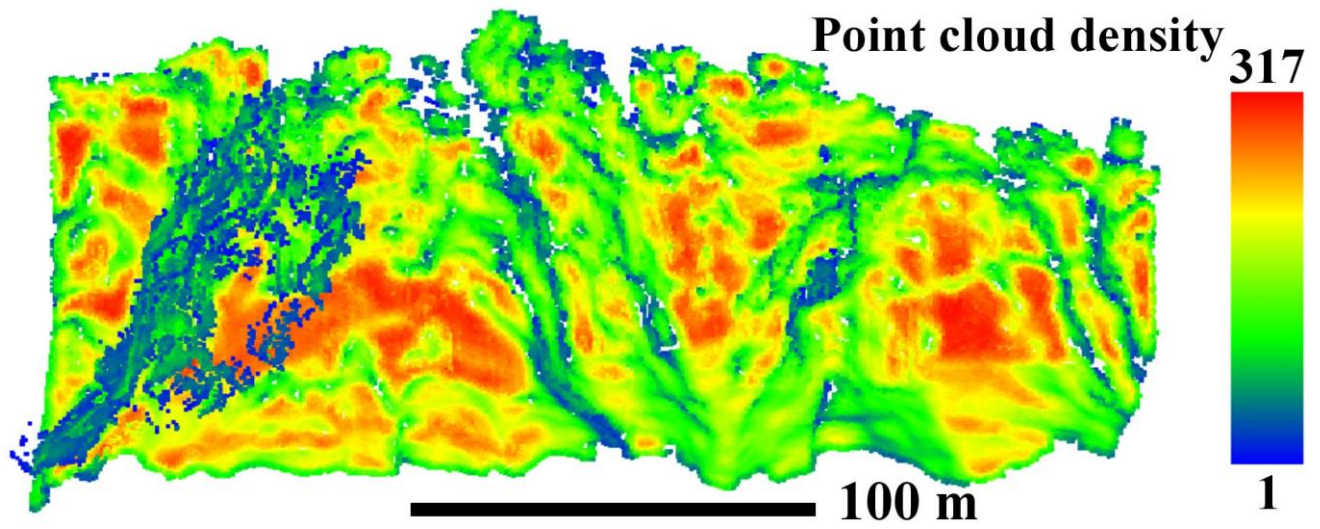


**Figure S4.** Point cloud density as computed in CloudCompare using a Kernel radius of 3 m.

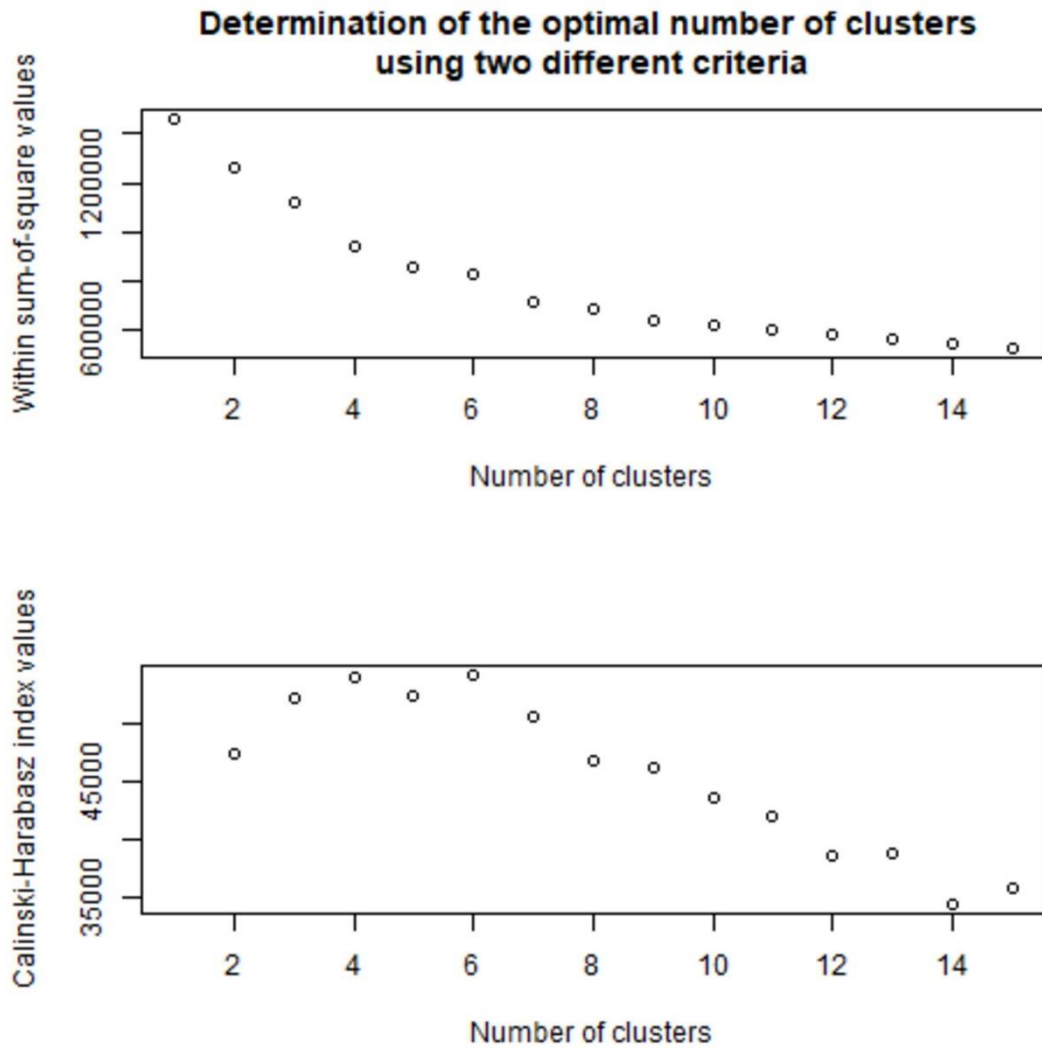


**Figure S5.** Plot of number of clusters against within sum of squares and Caliński-Harabasz criteria (Caliński and Harabasz, 1974). This allowed to select four abiotic clusters as being the optimal representation of the point cloud variability.

**Table S1.** Mean  $\pm$  standard deviation of abiotic variables calculated at different scales for each abiotic cluster computed by the K-means algorithm.

	Scale [m]	T1	T2	T3	T4
<b>Depth [m]</b>	0.3	-733 $\pm$ 19	-758 $\pm$ 22	-781 $\pm$ 26	-751 $\pm$ 27
<b>Backscatter [Nominal values]</b>	0.3	36.1 $\pm$ 7.2	53.4 $\pm$ 4.2	52.1 $\pm$ 4.2	50.1 $\pm$ 6.1
	0.9	37 $\pm$ 6.8	53.2 $\pm$ 3.8	52 $\pm$ 3.7	50 $\pm$ 5.6
<b>Slope [°]</b>	0.9	61 $\pm$ 18.4	70.9 $\pm$ 12.5	44.7 $\pm$ 12.6	61.9 $\pm$ 19.5
	3	59.6 $\pm$ 17.8	69.8 $\pm$ 9.6	43.1 $\pm$ 10	62.8 $\pm$ 18.3
	9	53.4 $\pm$ 15.4	64.6 $\pm$ 8.9	43.3 $\pm$ 7.9	57.3 $\pm$ 15
<b>BPI [10<sup>-2</sup> m]</b>	0.9	-0.73 $\pm$ 14.15	0.36 $\pm$ 8.34	0.09 $\pm$ 10.51	-0.52 $\pm$ 16.2
	3	-0.32 $\pm$ 38.46	1.75 $\pm$ 19.9	-2.3 $\pm$ 25.02	-2.59 $\pm$ 42.34
	9	21.05 $\pm$ 118.94	5.25 $\pm$ 74.1	-33.5 $\pm$ 88.08	-3.84 $\pm$ 110.93
<b>TRI [m]</b>	0.9	0.34 $\pm$ 0.07	0.37 $\pm$ 0.04	0.29 $\pm$ 0.06	0.34 $\pm$ 0.07
	3	1.05 $\pm$ 0.14	1.16 $\pm$ 0.07	0.9 $\pm$ 0.12	1.09 $\pm$ 0.11
	9	3.01 $\pm$ 0.38	3.33 $\pm$ 0.25	2.7 $\pm$ 0.33	3.14 $\pm$ 1.11
<b>Roughness [10<sup>-2</sup> m]</b>	3	28.69 $\pm$ 27.79	19.59 $\pm$ 23.33	18.09 $\pm$ 20.48	59.83 $\pm$ 36.31
	9	11.91 $\pm$ 15.97	7.52 $\pm$ 13.17	7.75 $\pm$ 12.59	28.45 $\pm$ 23.94
<b>Mean curvature [10<sup>-2</sup> m<sup>-1</sup>]</b>	3	6.06 $\pm$ 4.05	5.3 $\pm$ 3.75	5.05 $\pm$ 3.69	7.71 $\pm$ 4.18
	9	22.36 $\pm$ 17.97	15.14 $\pm$ 11.99	13.51 $\pm$ 11.73	41.63 $\pm$ 24.02

<b>Gaussian curvature</b> [10 <sup>-3</sup> m <sup>-1</sup> ]	3	12.94 ± 17.18	6.99 ± 8.66	4.72 ± 6.94	14.22 ± 18.33
	9	117.88 ± 144.45	57.51 ± 74.15	37.81 ± 60.98	243.94 ± 220.49
<b>Eastness [-]</b>	3	-0.52 ± 0.57	-0.61 ± 0.43	-0.59 ± 0.4	-0.41 ± 0.53
	9	-0.64 ± 0.43	-0.65 ± 0.38	-0.6 ± 0.37	-0.47 ± 0.46
<b>Northness [-]</b>	3	0.37 ± 0.52	0.51 ± 0.41	0.59 ± 0.38	0.54 ± 0.52
	9	0.46 ± 0.44	0.56 ± 0.34	0.61 ± 0.36	0.64 ± 0.38